

NGAO Laser Guide Star wavefront sensor : Type and
number of sub-apertures trade study

V. Velur
Caltech Optical Observatories
M/S 105-24, 1200 E California Blvd., Pasadena, CA 91125

January 29, 2007

Contents

1	Introduction:	3
2	Assumptions	3
3	Handling extended LGS with a SHWFS and a pyramid WFS	3
3.1	How a Shack Hartmann WFS can be made to handle elongated laser spots	4
3.2	How a pyramid sensor handles elongated spots	4
4	Pulse Tracking Options	4
4.1	Radial Geometry CCDs	4
4.2	Mechanical Resonator [6] [4] [5]	7
4.3	Other schemes	7
4.3.1	Cylindrical lens combination on a rotating wheel	7
4.3.2	MEMS resonator	8
5	Trade study results	8
6	Conclusions	9

List of Figures

1	Radial geometry CCD [1]	5
2	How elongated spots are handled and pulse tracking is implemented [1]	6
3	How elongated spots are handled and pulse tracking is implemented [2]	6
4	Narrow field case with a Shack Hartmann wavefront sensor	10
5	Narrow field case with a pyramid wavefront sensor	11
6	Wide field case with a SHWFS	12
7	Wide field case with a PWFS	13
8	Bad seeing and bad cirrus conditions	14

List of Tables

1	Table of assumed parameters	3
2	Comparison of different pulse tracking schemes	8
3	Table of Results for narrow field Shack Hartmann HOWFS, on axis TT star with 10% going to a slow WFS, TT star $m_v=19$	15
4	Table of Results for narrow field pyramid HOWFS, on axis TT star with 10% going to a slow WFS, TT star $m_v=19$	16
5	Table of Results for wide field Shack Hartmann HOWFS	17
6	Table of Results for wide field pyramid HOWFS	17

1 Introduction:

The Next Generation Adaptive Optics system (NGAO) is a multi-laser guide star adaptive optics system. This document looks at the advantages of accommodating multiple sub-apertures on the high order wavefront sensors and compares the performance of a pyramid and a Shack Hartmann based wavefront sensors. The merit is shown as wavefront error for different laser power levels and the laser power level assumed to be a cost driver. This is based on SEMP scope sheet which says "The WFS costs is not the issue (these are likely not a major driver); the significant cost driver between different numbers of subapertures is laser power".

WBS dictionary entry:

3.1.2.2.6 LGS Wavefront Sensor Type

Consider alternative WFS designs (e.g. Shack-Hartmann vs. pyramid) for different laser pulse formats. Evaluate and compare the advantages of e.g. short pulse tracking using radial geometry CCDs and mechanical pulse trackers. Complete when LGS WFS requirements have been documented.

3.1.2.2.7 LGS number of sub-apertures

Consider the cost/benefit of supporting different format LGS wavefront sensors (e.g. 44 subaps across, vs. 32, vs 24.) Consider the operational scenarios required to meet science requirements in poor atmospheric seeing or cirrus conditions.

2 Assumptions

Parameter	Value
Seeing (r_0)	0.180 arc-sec. at 0.5 μm at 0 deg. elevation
θ_0	2.50 arc-sec at 0 deg. elevation
Greenwood frequency (f_G)	39.43 Hz
Temperature	2.5 ± 4 deg. C
Wind speed	10 m/s
$f\#$	f/13.66 (10.949 m primary mirror)
LGS asterism configurations	Quincunx of 33 arcsec radius for wide field case and that of 10 arcsec radius for narrow field case
# of pixels/ sub-aperture on HOWFS	4

Table 1: Table of assumed parameters

3 Handling extended LGS with a SHWFS and a pyramid WFS

Beletic et. al. are developing a radial geometry CCD for a centrally launched CW laser. Not much work has been published on handling extended LGS sources using a pyramid sensor. But, Iglesias et. al. have developed a scheme to deal with extended sources using a pyramid sensor and proven the concept in the lab on low order aberrations using the human eye.

3.1 How a Shack Hartmann WFS can be made to handle elongated laser spots

The AODP and CARA funded project to develop low noise CCD detectors with a planar JFET based amplifier on a back-thinned device (CCID-56b) has been showing promising results. The noise estimates from these rectilinear CCDs is very encouraging ($1 e^-$ RON at 1 MHz pixel rate). The radial versions of these devices, as shown in figures 1-2, will be well suited to handle a CW laser spots that are centrally projected. To reduce centroiding error due to elongated spots either a noise optimal centroiding algorithm or a matched filter scheme can be used in conjunction with a radial CCD with pixels as large as 2×8 arcsec near the circumference of the detector.

3.2 How a pyramid sensor handles elongated spots

The only reference that I could find on this subject suggests that a PWFS can handle an extended source and to first order the sensitivity of the system is twice as high as a regular point source. The paper has no SNR calculations. More effort needs to go into modeling the PWFS to understand the exact SNR while using it with an extended laser beacon. This trade study assumes that there is no lenslet diffraction effect in case of the PWFS for WFE calculations and there is no guide star sharpening of any kind in the model.

4 Pulse Tracking Options

The ultimate laser for LGS AO is a laser for mitigating both Rayleigh back scatter and fratricide is to have a $1-3 \mu\text{sec}$ laser with a rep. rate of about 50KHz. With this kind of a pulsed laser the WFS needs to track the laser pulse as it traverses the 10Km long Na-layer, hence the need for pulse trackers. Pulse tracking can be done using a CCD (purely electronic), using macroscopic mechanical resonators, cylindrical lens combinations and using a MEMS resonator. The first two methods are being actively pursued by the astronomical AO community. There is already a working resonator that tracks Rayleigh beacons.

4.1 Radial Geometry CCDs

These CCDs are built to be able to sample LGS light on large telescopes. They are built so that they can either accommodate an extended LGS spot or integrate on a moving spot by transferring the charge along with the spot motion on the FPA. The CCD is equipped with clock lines that enable this process. Each sub-aperture has image and charge transfer areas with dump drain capability with 3 phase programmable clocks. The aim of the AODP program is to develop a device that has 20 amplifiers and can run at 2KHz (in 2×2 pixel(binned)/sub-aperture mode) with less than $3 e^-$ of read noise. The current success of lab tests show that sub-electron read noise may be achievable with these devices if the planar JFET architecture of their back-thinned devices give the performance as the model and the rectilinear device tests show.

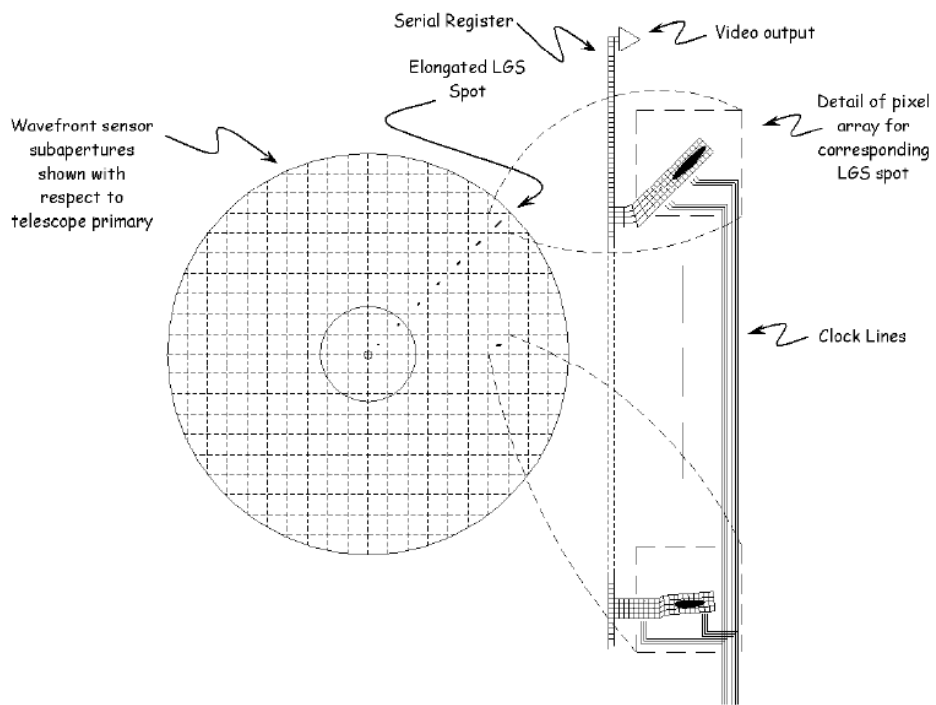


Figure 1: Radial geometry CCD [1]

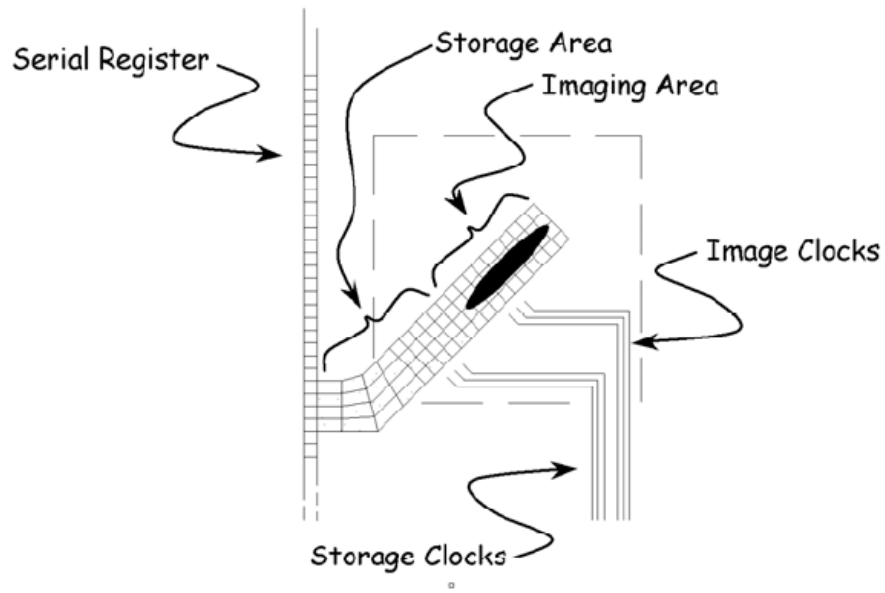


Figure 2: How elongated spots are handled and pulse tracking is implemented [1]

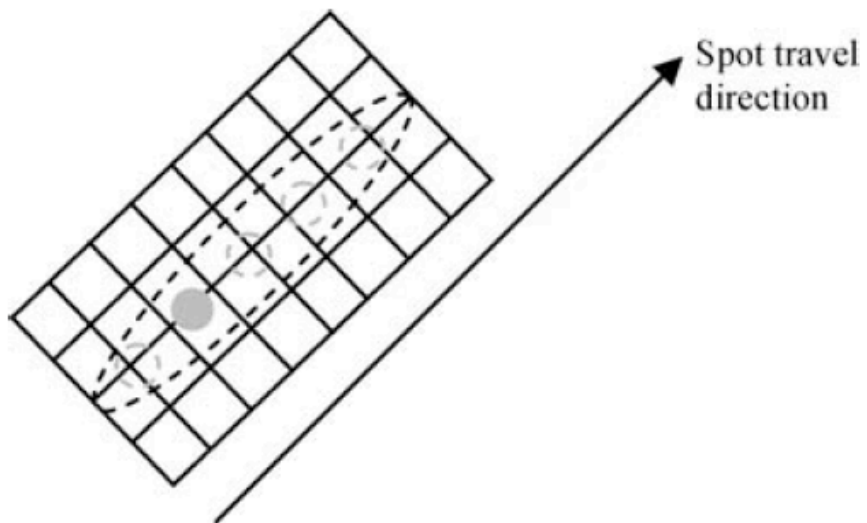


Figure 3: How elongated spots are handled and pulse tracking is implemented [2]

4.2 Mechanical Resonator [6] [4] [5]

Commercial resonators and drive electronics are available to build a mechanical resonator for tracking LGS pulses, since ultrasonic welding of plastics is done very using similar equipment. Krell Engineering is a custom resonator manufacturer that builds resonators using 6Al14V Titanium alloy or some similar aluminum alloy. The geometry of the resonator may be step, exponential or a hybrid horn with active cooling. We may have to give the resonator manufacturer the mirror specification (size, weight, density, geometry etc.), and we have to figure out a bonding technique that will withstand ultrasonic operation. The basic principle is to use a fatigue resistant material with sufficiently high heat conduction to build a high Q resonator. The natural frequency of the horn (resonator) is a design parameter and is chosen to be as close as possible to the operating frequency. The horn is a tapered piece of metal with a transducer that induces strain on the bigger end and this translates into a amplified strain on the smaller end. This strain is manifested as a mirror motion if a mirror is attached at the smaller end.

For example, a 20 KHz resonator is 5" in length and 3" at the transducer end and 0.25" at the output. The size for a 50 KHz resonator is approximately $\frac{2}{5}$ th. The lower the natural frequency the greater the amplitude obtained from the resonator. Typical amplitudes obtained from a 20 KHz resonator is 300 microns. So a 50 KHz resonator will yield a stroke of 120 microns. A optical design is for a suitable objective that converts the focus shift from the AO focus shift to something that can be actively tracked by the mechanical resonator is presented by Georges et. al. [6], but has 14 additional surfaces to dynamically refocus the LGS spots.

The cost of the resonator is between \$2500 - \$3500 (depending on complexity). There are multiple vendors for drive electronics (Branson Ultrasonics, Sonics and Materials etc.) and the cost for the electronics is about \$4000. These units consume about 2KW of power.

$$\Delta z' = \Delta z \frac{f}{(f + z)} \quad (1)$$

where,

$\Delta z'$ - change in focus after the telescope (m)

Δz - the Rayleigh range gate (m)

f - Effective focal length of the optical system (m)

z - center of the range gate (m)

$$\Delta z' = 15.764 \text{ mm.}$$

An effective objective that converts this to 120 μ m or less of travel will need to be designed. Georges et. al. describe a scheme to design a suitable objective for this application.

4.3 Other schemes

4.3.1 Cylindrical lens combination on a rotating wheel

A combination of a set of 2 cylindrical lenses with varying radius curvature made as a arc of a circle can be mounted on rotary wheels to be able to track the sodium beacon.

4.3.2 MEMS resonator

Don Gavel has talked to Boston Micromachines (MEMS mirror manufacturer) about the possibility of using a MEMS membrane mirror to track laser pulses. Paul Bierden suggests that it is possible to make MEMS structures that have a natural frequency large enough to support 50 KHz operation, but according to BMM it is possible to only produce a tilt with this kind of a structure and not a pure translation.

A comparison of the different pulse tracking schemes is shown in table 2.

Tracking scheme	Cost (when mature)	Complexity	Notes
Radial geo. CCD	paid for by AODP	electronics	works only for SHWFS with lasers projected from the center
Mechanical resonator	\$10,000	ultrasonics used at MMT on Rayleigh beacons	Currently tested optical design has 14 extra surfaces
Cylindrical lenses on rotating disc	\$10,000	needs prototyping	still at conceptual level
MEMS mirror	???	needs prototyping	still at conceptual level

Table 2: Comparison of different pulse tracking schemes

5 Trade study results

The performance benefit vs. cost (laser power) was done using Rich Dekany's WFE spreadsheet with the general assumptions described in the assumptions section. Additional assumptions and parameters were used to simulate the following science observing scenarios:

The atmosphere used was based on KAON 303 (Chris Neyman's atmosphere) and pixel charge diffusion was assumed to be 0.3 pixels for the SHWFS case. With a PWFS, the charge diffusion was assumed to be zero charge diffusion and the AO spot size was used instead of the lenslet-diffracted on spot size. No MEMS mirror based active correction of the spot size at the WFS was considered.

1. Narrow field case with a Shack Hartmann wavefront sensor - additional assumptions: On-axis TT star with 10 percent light going to a slow WFS, TT star $m_v = 19$ or dimmer, SCAO, LGS quincunx radius=5 arcsec. The charge diffusion was assumed to be 0.3 pixels. H-band Strehl was optimized by varying the TT and HOWFS loop rates for various 3 sets of sub-apertures and various laser power levels.
2. Narrow field case with a pyramid wavefront sensor - On-axis TT star with 10 percent light going to a slow WFS, TT star $m_v = 19$, SCAO, LGS quincunx radius=5 arcsec. H-band Strehl was optimized by varying the TT and HOWFS loop rates for various 3 sets of sub-apertures and various laser power levels.

3. Wide field case with a Shack Hartmann WFS - Sky coverage set to 15 percent. There are 2 TT stars with 10 percent of the light from the brightness one feeding a slow WFS. The Spagna sky model was used to find TT stars. The correction is perfect (tomography error is modeled separately) if the TT stars are inside the quincux and if the TT stars are outside they suffer anisoplanatism. The LGS asterism size was set to 33 arc-sec as suggested in KAON 429. Worst case tomography error from KAON 429 was used. I optimized HO integration time, TT int. time, TT guide star brightness (at the cost of search radius) to optimize H band Strehl for various 3 sets of sub-apertures and various laser power levels.
4. Wide field case with a pyramid WFS - Sky coverage was fixed at 15 percent. There are 2 TT stars with 10 percent of the light from the brightness one feeding a slow WFS. The Spagna sky model was used to find TT stars. The correction is perfect (tomography error is modeled separately) if the TT stars are inside the quincux and if the TT stars are outside they suffer anisoplanatism. The LGS asterism size was set to 33 arc-sec as suggested in KAON 429. Worst case tomography error from KAON 429 was used. I optimized HO integration time, TT int. time, TT guide star brightness (at the cost of search radius) to optimize H band Strehl for various 3 sets of sub-apertures and various laser power levels. Charge diffusion was assumed to be zero charge diffusion and the AO spot size was used instead of the lenslet-diffracted on spot size.
5. Narrow field case with both Shack Hartmann and pyramid WFS's in case of bad seeing and bad cirrus clouds -
 Narrow field case with SHWFS and PWFS with poor seeing- $r_0=0.10$ m, wind velocity = 15 m/s, laser power = 150W
 Narrow field case with SHWFS and PWFS with poor seeing and Cirrus conditions- $r_0=0.10$ m, wind velocity = 15 m/s, laser power = 50W. For simulating this case I just reduced the laser power but didn't account for the extra scatter on the WFS due to the extinction that would be seen in case of cirrus clouds. The scatter information will be available after the Rayleigh rejection trade study is complete.
6. For the wide field case the WFE in case of bad seeing and cirrus is 610 nm (561 nm high order of which 470nm is contribution from LGS tomography and 240 nm of tip-tilt error) and that in case of bad seeing and no cirrus is 567nm (518nm high order of which 470nm is contribution from LGS tomography and 232 nm of tip-tilt error).

I plot WFE vs. # of sub-apertures for laser power levels of 50, 100, 150 and 200W for the above mentioned conditions.

6 Conclusions

- If we are going to be using a CW laser it is best to work with a SHWFS and a radial geometry CCD. Both technologies are mature (as compared to counterparts) and the advantage of PWFS is only a few (less than 5 nm) nm in WFE as presented by current models.
- In the wide field cases the majority of the error (288 nm) comes from tomography.
- With a pulsed laser, still the option of SHWFS with a radial format CCD, seems like the simplest and most efficient way to proceed w.r.t pulse tracking. The contingency plan will be to use macroscopic mechanical resonator based pulse trackers.

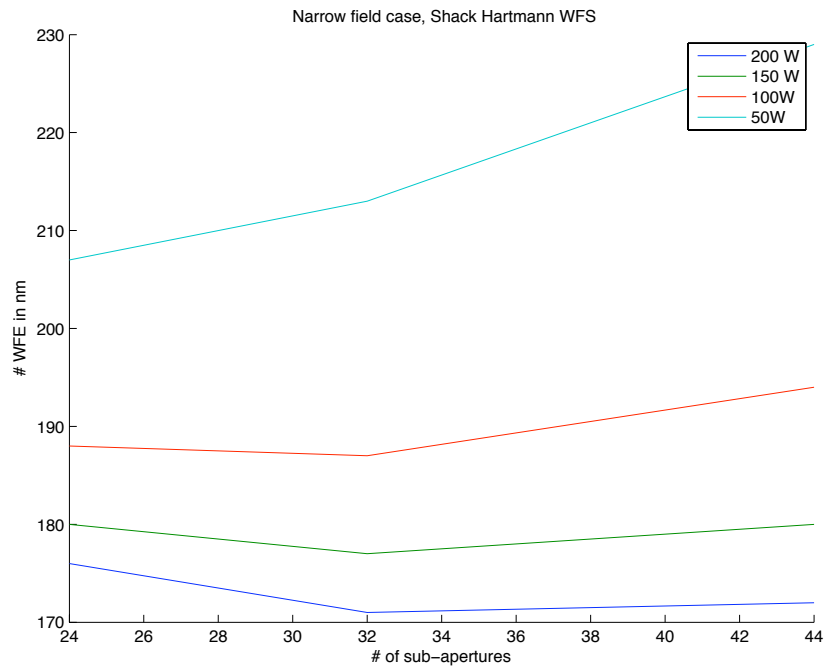


Figure 4: Narrow field case with a Shack Hartmann wavefront sensor

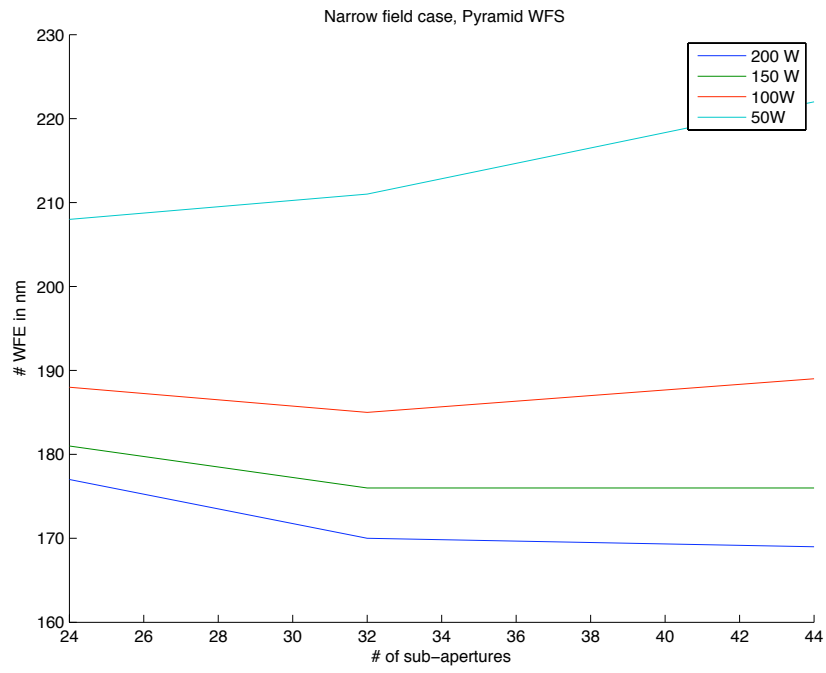


Figure 5: Narrow field case with a pyramid wavefront sensor

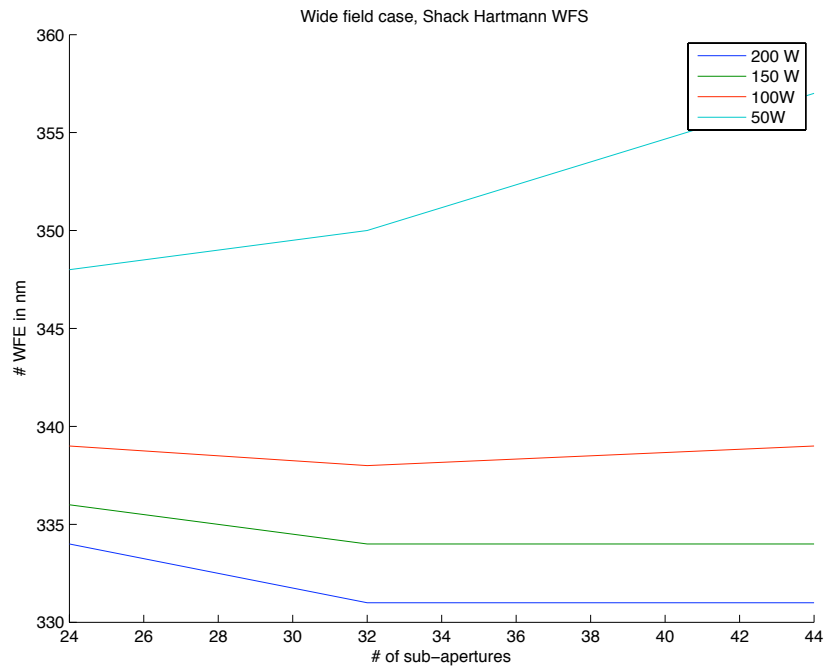


Figure 6: Wide field case with a SHWFS

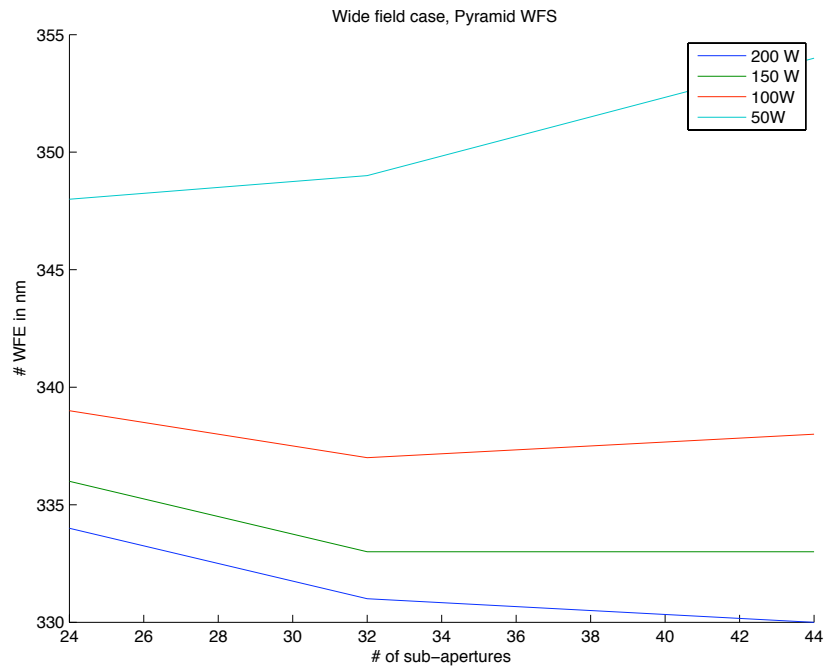


Figure 7: Wide field case with a PWFS

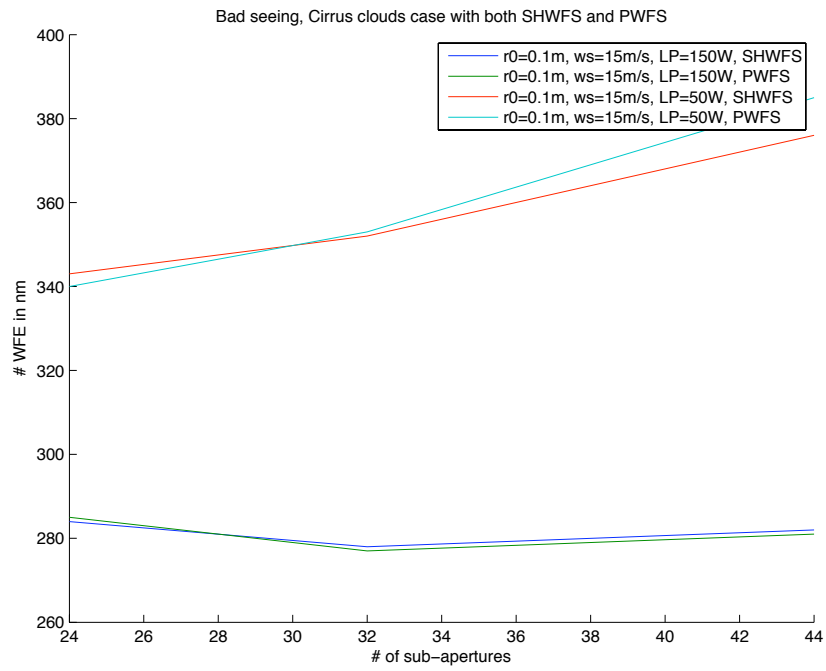


Figure 8: Bad seeing and bad cirrus conditions

Laser power(W)	# of sub-apertures	TTWFE (nm)	HOWFE (nm)	Total WFE(nm)
200	44	91	146	172
200	32	91	141	171
200	24	92	151	176
150	44	93	154	180
150	32	92	151	177
150	24	93	155	180
100	44	95	169	194
100	32	94	161	187
100	24	94	163	184
50	44	102	205	229
50	32	99	189	213
50	24	98	183	207

Table 3: Table of Results for narrow field Shack Hartmann HOWFS, on axis TT star with 10% going to a slow WFS, TT star $m_v=19$

- It is useful to have the option of multiple sub-apertures only in case of low laser power at the 50W level. Otherwise there is only a few nm of WFE difference between the 32 sub-apertures and 44 sub-aperture case. The 24 sub-aperture case performs badly except for the 50W laser power case. Depending on the laser source choice, the EC must make a choice of either 24 and 32 sub-apertures or 32 and 44 sub-apertures if the incremental cost or packaging constraint of supporting 3 lenslet gets to be too much work. **For calibration and DM registration purposes it may be useful to support a 64x64 sub-aperture mode.**
- In case of bad seeing and cirrus cloud conditions it is best that only narrow field science must be performed and 32 sub-aperture case gives optimal performance for both cases. There is no significant difference between the PWFS and SHWFS case. For the wide field case the WFE in case of bad seeing and cirrus is 610 nm and that in case of bad seeing and no cirrus is 567nm. The split up of the error terms is stated in the results section.

Laser power(W)	# of sub-apertures	TTWFE (nm)	HOWFE (nm)	Total WFE(nm)
200	44	91	143	169
200	32	91	144	170
200	24	92	151	177
150	44	92	150	176
150	32	92	150	176
150	24	93	155	181
100	44	94	164	189
100	32	94	160	185
100	24	94	163	188
50	44	101	198	222
50	32	98	187	211
50	24	98	184	208

Table 4: Table of Results for narrow field pyramid HOWFS, on axis TT star with 10% going to a slow WFS, TT star $m_v=19$

References

- [1] B. Bauman, PhD Thesis.
- [2] J Beletic et. al., The ultimate CCD for laser guide star wavefront sensing on extremely large telescopes.
- [3] I Igelesias et. al., Extended source pyramid wavefront sensor for the human eye., Optics Express, Vol. 10, No.9, Pg. 419.
- [4] Krell Engineering, Private communication.
- [5] Branson Ultrasonics, Private communication.
- [6] J. A. Georges et. al., Design and testing of a dynamic refocus system for Rayleigh laser beacons, Adaptive Optical System Technologies II, (Proc. SPIE), eds. P. L.Wizinowich, & D. Bonaccini, 4839, 473 (2002).

Laser power(W)	# of sub-apertures	TTWFE (nm)	HOWFE (nm)	Total WFE(nm)
200	44	107	313	331
200	32	107	313	331
200	24	107	316	334
150	44	107	313	334
150	32	107	316	334
150	24	108	318	336
100	44	108	322	339
100	32	108	320	338
100	24	108	322	339
50	44	109	340	357
50	32	108	333	350
50	24	108	331	348

Table 5: Table of Results for wide field Shack Hartmann HOWFS

Laser power(W)	# of sub-apertures	TTWFE (nm)	HOWFE (nm)	Total WFE(nm)
200	44	107	312	330
200	32	107	313	331
200	24	107	316	334
150	44	107	315	333
150	32	107	315	333
150	24	108	318	336
100	44	108	321	338
100	32	108	320	337
100	24	108	322	339
50	44	109	337	354
50	32	108	332	349
50	24	108	331	348

Table 6: Table of Results for wide field pyramid HOWFS